ISSN 2394-3777 (Print)
ISSN 2394-3785 (Online)
Available online at www.ijartet.com

International Journal of Advanced Research Trends in Engineering and Technology (IJARTET)
Vol. 5, Special Issue 12, April 2018

IMPLEMENTATION OF MODIFIED SOLAR PANEL PHOTOVOLTAIC GRID CONNECTED PV SYSTEM

C.Selsiya

M.E., PED, P. A College of engineering and technology,Pollachi,India

Abstract: **Photovoltaic (PV) generators are a good option for producing electricity in a decentralized and sustainable way. The development of enhanced power electronic interfaces and training of HQP is still in high demand. This paper discusses the digital implementation of the required control loops of a typical 2-stage PV interface using a low power renewable energy developer's kit (REK).Experimental results demonstrate the effectiveness of the selected techniques and implementation in steady-state and transient conditions.**

Keywords: ***renewable energy; PV inverter; digital control;MPPT; grid-connected; stand-alone.***

INTRODUCTION

PV systems interfaces are based on power electronic converters [1], [2], [3]. They can be connected to the conventional utility grid or installed in autonomous (standalone) systems, also known as mini-grids. Since their required features can vary significantly, depending on the application, it is very convenient to use a flexible platform for controlling the power interfaces. A number of low-cost digital signal processors (DSPs) that present the resources necessary for implementing the control structure of PV inverters. One of them is the Texas Instruments C2000 family of microcontrollers with its enhanced peripheral set and optimized CPU core for control tasks.

Digital control logic for PV interfaces with similar systems have been presented in the literature, many do not provide experimental results [5]. This paper focuses on the digital implementation of the various control loops required for a typical storage-less 2-stage (DC-DC and DC-AC) PV interface using the TI Renewable Energy Developer's Kit. The control system comprises a maximum power point tracking (MPPT) algorithm that allows the boost DC-DC converter to draw the maximum amount of power available in a PV panel and that varies with the solar irradiance, cell temperature and so on [6]. A simple logic for preventing overvoltage in the intermediate DC bus, when the load demand is low in the stand-alone mode or when the grid is

General Specifications Of the solar module are as follows:

Capacity of Plant:100 KW
Cost of Plant: 79.49 Lacs INR
Daily Power Generation:400-450 KWH (On Sunny Days)

Annual Power Generation: 1, 50,000 Units

Solar PV module *and* ***Inverter*** are two important constituents of the Photovoltaic energy system. Online real time access to the generation dataand performance specifications is also available with help of interconnected local area network.

Awareness for social change

It will be helpful in creating awareness in young minds present inUniversity which acts as a hub for exchanging ideas, information and awareness in society for such initiatives of clean energy

environment friendly

As an initiative towards green campus it will be helpful in cutting down dependence on conventional energy as well as

ISSN 2394-3777 (Print)
ISSN 2394-3785 (Online)
Available online at www.ijartet.com

International Journal of Advanced Research Trends in Engineering and Technology (IJARTET)
Vol. 5, Special Issue 12, April 2018

it will contribute towards carbon credit control and control of pollution.

Research & Development

It will be helpful for understanding the theory and applications of rooftop Solar PV system. Detailed case study, reports, research ideas and new development can be formulated using such a system in University.

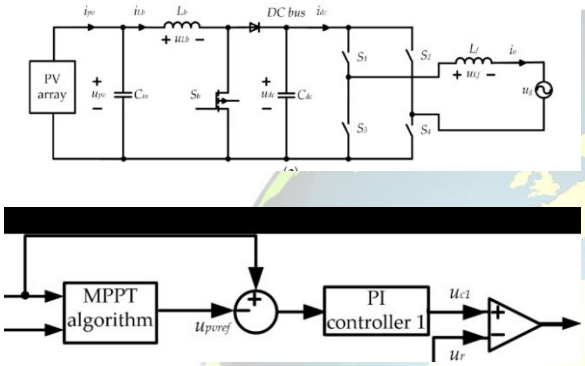

pv Array

The output current ipv of the PV array is related to the output voltage upv and also affected by other parameters of PV panel itself [25]. However, the manufacturer's datasheet do not provide some of these parameters, such as equivalent series resistance and equivalent parallel resistance. Basic parameters provided in all datasheets of PV array are open circuit voltage UOC, short circuit current ISC, the current at maximum power point (MPP) IM, and the voltage at maximum power point UM. These parameters are all with the standard test condition (STC). To overcome the lack of detailed information of the PV array, a simplified model proposed in [26] is used in this study, which describes the terminal characteristic of the PV array with STC.

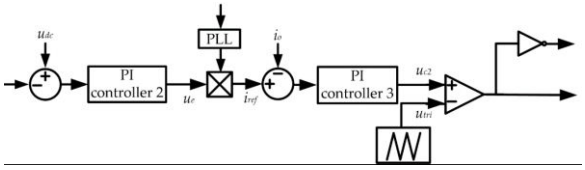

power stage circuit

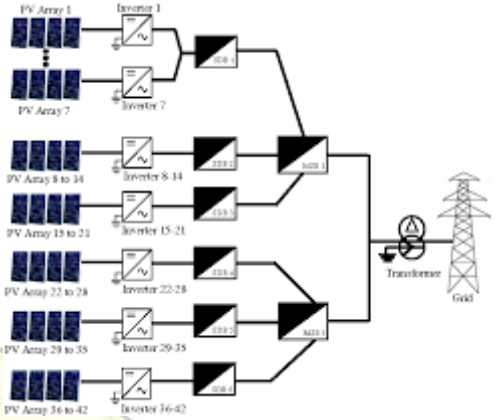

To describe the power stage circuit, four sate variables are used: the output voltage of PV array upv, the current of Lb which denoted as iLb , the DC bus voltage udc and the output current of full bridge inverter io. The averaged equations of the input filter and boost converter can be derived as follows [19]:

$$i_{pv} = I_{SC}\left[1 - A_1\left(e^{\frac{u_{pv}}{A_2 U_{OC}}} - 1\right)\right]$$

where $A_1 = \left(1 - \frac{I_M}{I_{SC}}\right)e^{-\frac{U_M}{A_2 U_{OC}}}$, $A_2 = \left(\frac{U_M}{U_{OC}} - 1\right)\left[ln\left(1 - \frac{I_M}{I_{SC}}\right)\right]^{-1}$.

According to the operation principle of the full bridge inverter, following equations can be derived

$$\begin{cases} i_{dc} = (2d_2 - 1)i_o \\ \frac{di_o}{dt} = \frac{1}{L_f}\left[(2d_2 - 1)u_{dc} - u_g\right] \end{cases}$$

then the averaged equations of the power stage circuit

$$\begin{cases} \frac{du_{pv}}{dt} = \frac{1}{C_{in}}\left(i_{pv} - i_{L_b}\right) \\ \frac{di_{L_b}}{dt} = \frac{1}{L_b}\left[u_{pv} - (1 - d_1)u_{dc}\right] \\ \frac{du_{dc}}{dt} = \frac{1}{C_{dc}}\left[(1 - d_1)i_{L_b} - (2d_2 - 1)i_o\right] \\ \frac{di_o}{dt} = \frac{1}{L_f}\left[(2d_2 - 1)u_{dc} - u_g\right] \end{cases}$$

ISSN 2394-3777 (Print)
ISSN 2394-3785 (Online)
Available online at www.ijartet.com

International Journal of Advanced Research Trends in Engineering and Technology (IJARTET)
Vol. 5, Special Issue 12, April 2018

The state equations corresponding to the Proportional-Integral (PI) controller can be expressed as follow

$$\frac{dm(t)}{dt} = K_p \frac{de(t)}{dt} + \frac{K_p}{T_i} e(t)$$

where m(t) and e(t) are the output and the input signals of the PI controller, respectively, Kp is the gain of the PI controller, and Ti is the time constant of the PI controller.

Since the perturbation step size of P&O method is small, the reference voltage upvref given by the algorithm is assumed to be constant.

$$\frac{du_{c1}}{dt} = K_{p1} \frac{du_{pv}}{dt} + \frac{K_{p1}}{T_{i1}} \left(u_{pv} - u_{pvref} \right)$$

where uc1 is the output signal of PI controller 1 and Kp1 and Ti1 are the gain and the time constant of the PI controller. uc1 is compared to a ramp ur in the PulseWidth Modulation (PWM) comparator to produce driving signal. To complete the model of MPPT controller, the duty cycle d1 is expressed as following equation:

$$d_1 = \frac{u_{c1}}{U_{M1}}$$

where UM1 is the peak-to-peak amplitude of ramp ur.

The state equation of PI controller 2 can be derived as

$$\frac{du_e}{dt} = K_{p2} \frac{du_{dc}}{dt} + \frac{K_{p2}}{T_{i2}} \left(u_{dc} - u_{dcref} \right)$$

udcref is the reference voltage of DC bus, ue is the output signal of PI controller 2, Kp2 and Ti2 is the gain and the time constant of the PI controller.

The nonlinear averaged equations of the system

$$\begin{cases} \frac{du_{pv}}{dt} = \frac{1}{C_{dc}} \left(I_{SC} \left[1 - A_1 \left(e^{\frac{u_{pv}}{A_2 U_{OC}}} - 1 \right) \right] - i_{L_b} \right) \\ \frac{di_{L_b}}{dt} = \frac{1}{L_b} \left[u_{pv} - \left(1 - \frac{u_{c1}}{U_{M1}} \right) u_{dc} \right] \\ \frac{du_{dc}}{dt} = \frac{1}{C_{dc}} \left[\left(1 - \frac{u_{c1}}{U_{M1}} \right) i_{L_b} - \frac{u_{c2} i_o}{U_{M2}} \right] \\ \frac{di_o}{dt} = \frac{1}{L_f} \left[\frac{u_{c2}}{U_{M2}} u_{dc} - U_{gm} sin(\omega t) \right] \\ \frac{du_{c1}}{dt} = K_{p1} \frac{du_{pv}}{dt} + \frac{K_{p1}}{T_{i1}} \left(u_{pv} - u_{pvref} \right) \\ \frac{du_e}{dt} = K_{p2} \frac{du_{dc}}{dt} + \frac{K_{p2}}{T_{i2}} \left(u_{dc} - u_{dcref} \right) \\ \frac{du_{c2}}{dt} = K_{p3} \left(u_e \omega cos(\omega t) + sin(\omega t) \frac{du_e}{dt} - \frac{di_o}{dt} \right) + \frac{K_{p3}}{T_{i3}} (u_e sin(\omega t) - i_o) \end{cases}$$

Observer-Pattern Model

The equations shown in (12) contain sin(*w*t) and cos(*w*t), which means that the single-phase two-stage grid-connected photovoltaic system is a time-variant nonlinear system. This time-variance is the main difficulty in stability analysis of the system. To eliminating the effect of time-variance, the system is transformed into a time-invariant one using an observer-pattern modeling method [21,22]. Notice that sin(*w*t) and cos(*w*t) only exist in the expressions of dio/dt and duc2/dt. Thus, only io and uc2 need to be processed.

$$\begin{cases} i_{odq} = \begin{bmatrix} i_{od} \\ i_{oq} \end{bmatrix} = \boldsymbol{T} \begin{bmatrix} i_o \\ i_{oI} \end{bmatrix} \\ u_{c2dq} = \begin{bmatrix} u_{c2d} \\ u_{c2q} \end{bmatrix} = \boldsymbol{T} \begin{bmatrix} u_{c2} \\ u_{c2I} \end{bmatrix} \end{cases}$$

first, the time-variance originated from fundamental frequency of the grid is removed by Park transformation. Implementation of Park transformation needs at least two orthogonal variables, so the concept of Imaginary Orthogonal Circuit is introduced [27]. Denote the corresponding Imaginary Orthogonal Circuit variables to io and uc2 as ioI and uc2I. Since io and uc2 are sinusoidal, ioI and uc2I maintain 90_ phase shift with io and uc2. The Park transformation can be expressed as

ISSN 2394-3777 (Print)
ISSN 2394-3785 (Online)
Available online at www.ijartet.com

International Journal of Advanced Research Trends in Engineering and Technology (IJARTET)
Vol. 5, Special Issue 12, April 2018

$$
\begin{cases}
\frac{du_{pv}}{dt} = \frac{1}{C_{in}}\left(I_{SC}\left[1 - A_1\left(e^{\frac{u_{pv}}{A_2 U_{OC}}} - 1\right)\right] - i_{L_b}\right) \\
\frac{di_{L_b}}{dt} = \frac{1}{L_b}\left[u_{pv} - \left(1 - \frac{u_{c1}}{U_{M1}}\right)u_{dc}\right] \\
\frac{du_{dc}}{dt} = \frac{1}{C_{dc}}\left[\left(1 - \frac{u_{c1}}{U_{M1}}\right)i_{L_b} - \frac{1+g_1}{2}u_{c2d}i_{od} - \frac{1-g_1}{2}u_{c2q}i_{oq} + \frac{g_2}{2}\left(u_{c2d}i_{oq} + u_{c2q}i_{od}\right)\right] \\
\frac{di_{od}}{dt} = \frac{u_{dc}u_{c2d}}{L_f U_{M2}} + \omega i_{oq} \\
\frac{di_{oq}}{dt} = \frac{u_{dc}u_{c2q}}{L_f U_{M2}} + \frac{U_{gm}}{L_f} - \omega i_{od} \\
\frac{du_{c1}}{dt} = K_{p1}\frac{du_{pv}}{dt} + \frac{K_{p1}}{T_{i1}}\left(u_{pv} - u_{pvref}\right) \\
\frac{du_e}{dt} = K_{p2}\frac{du_{dc}}{dt} + \frac{K_{p2}}{T_{i2}}\left(u_{dc} - u_{dcref}\right) \\
\frac{du_{c2d}}{dt} = K_{p3}u_e\omega - \frac{K_{p3}}{L_f U_{M2}}u_{dc}u_{c2d} - \frac{K_{p3}}{T_{i3}}i_{od} + \omega u_{c2q} \\
\frac{du_{c2q}}{dt} = -K_{p3}\frac{du_e}{dt} - \frac{K_{p3}}{L_f U_{M2}}u_{dc}u_{c2q} - \frac{U_{gm}K_{p3}}{L_f} - \frac{K_{p3}}{T_{i3}}u_e - \frac{K_{p3}}{T_{i3}}i_{oq} - \omega u_{c2d} \\
\frac{dg_1}{dt} = -2\omega g_2 \\
\frac{dg_2}{dt} = 2\omega g_1
\end{cases}
$$

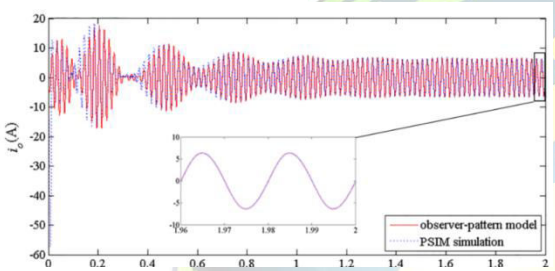

Stability Analysis

The gain and the time constant of three PI controllers are key parameters that affect the performance of the system. As these parameters change, the eigenvalues of the system also change. For the purpose of estimating the direction and size of the eigenvalue movement due to variations in system parameters, a sensitivity analysis is often used [28,29].

The decrease in Kp3 makes *l*1,2 move toward right in the s-plane. For *l*3,4, the most sensitive parameters are Ti1 and Kp1. A negative perturbation in Ti1 makes *l*3,4 move towards right in the s-plane. In contrast, the decrease in Kp3 makes *l*3,4 move to left. For *l*5, the most critical parameter is Ti1. The increase in Ti1 leads to *l*5 moving towards right-half plane. For *l*6,7, the most sensitive parameter is Kp2. When Kp2 decreases, *l*6,7 moves towards right in the s-plane. For *l*8,9, the most sensitive parameters is Ti3. The increase in Ti3 leads to *l*8,9 moving towards right in the s-plane.

	$\lambda_{1,2}$	$\lambda_{3,4}$	λ_5	$\lambda_{6,7}$	$\lambda_{8,9}$	$\lambda_{10,11}$
K_{p1}	$-8.93 \times 10^{-4} \pm j7.47 \times 10^{-6}$	$5.57 \pm j1.38 \times 10^{4}$	-9.31	$-0.91 \pm j0.145$	$-2.45 \times 10^{-5} \pm j2.42 \times 10^{-4}$	0
T_{i1}	$-2.78 \times 10^{-7} \pm j2.88 \times 10^{-9}$	$-47.5 \pm j0.21$	94.9	$0.0286 \pm j0.193$	$3.85 \times 10^{-6} \pm j3.28 \times 10^{-7}$	0
K_{p2}	$-937 \pm j35.6$	$-0.605 \pm j0.188$	-0.664	$-134 \pm j553$	$0.00347 \pm j0.00126$	0
T_{i2}	$-11.8 \pm j0.68$	$-0.0211 \pm j0.0846$	1.47	$11 \pm j1.144$	$1.22 \times 10^{-4} \pm j0.00224$	0
K_{p3}	$-1.6 \times 10^{4} \pm j0.977$	$7.45 \times 10^{-4} \pm j0.00145$	-1.35×10^{-4}	$0.236 \pm j0.0336$	$0.00154 \pm j0.00409$	0
T_{i3}	$-25 \pm j7.68 \times 10^{-4}$	$2.62 \times 10^{-5} \pm j1.36 \times 10^{-5}$	2.21×10^{-5}	$0.00141 \pm j0.0192$	$25 \pm j0.0208$	0

This section provides a background on the control strategies used in the two power converters of the PV interface when connected to the grid and when supplying an isolated (stand-alone) load or system. *A.*

MPPT Algorithm

There are many maximum power point tracking (MPPT) techniques for PV systems [8]. In this work a method called "Perturb and Observe" (P&O) has been selected because of its ease of implementation and overall good performance. The parameter that will be used to introduce the disturbance in the system is the duty cycle (*D*) of the boost DC-DC converter. In this way, the operating point of the PV panel will be bouncing around the maximum power point (MPP) as the solar irradiance reaches a steady-state condition.

Inverter Control in Grid-Connected Mode

In most cases, a PV interface is connected to an AC power grid, as shown in Fig. 3. It is controlled so as to inject the maximum power available in the PV panel into the grid, with unity power factor (UPF). In such a case, the boost DCDC converter operates with MPPT and the DC-AC converter operates as a current source,injecting current in phase with the grid voltage. The magnitude of the reference current of the DC-AC converter is adjusted so as to regulate the magnitude of the voltage in the intermediate DC bus. This is shown in Fig. 3 where the conventional SPWM scheme with cascaded outer-voltage loop and inner-current loop is used. Linear PI-type controllers are used in both loops. A feedforward loop to minimize the impact of the grid voltage in the AC current waveform is also employed.

Inverter Control in Stand-Alone Mode

In some applications, the PV interface might be required to supply an isolated AC load, where it has to regulate the magnitude and the frequency of the output/load voltage. This

ISSN 2394-3777 (Print)
ISSN 2394-3785 (Online)
Available online at www.ijartet.com

International Journal of Advanced Research Trends in Engineering and Technology (IJARTET)
Vol. 5, Special Issue 12, April 2018

can be done with a control scheme similar to that shown in Fig. 4, but with the outer-voltage loop being used to regulate the AC voltage across the load. In such a case, the voltage in the intermediate DC bus would vary depending in the unbalance of the input (PV) and the output (load) powers of the system.

Results

The schematic diagram of the experimental set-up used in this paper is shown in Fig. 4 and Fig. 5. It can be used to test grid-connected and autonomous inverter operation. The solar array simulator (SAS) model E4350B (AGILENT) was used to emulate a PV panel with characteristics suitable to be used with the TI REK. These parameters, listed in Table 2 were programmed into the SAS with a dedicated PC. A number of tests were conducted for verifying the performance of the control strategies and implementation approaches described in the previous section.

Operation in the Grid-Connected Mode

In this mode, the boost DC-DC converter operates with MPPT, drawing as much power available in the PV panel as possible, which varies as a function of the solar iradiance. The DC-AC converter operates with unity power factor (UPF) injecting the amount of active power required to regulate the intermediate DC bus voltage. Fig. 6 depicts the waveforms of the voltage and current of the PV panel with the P&O MPPT technique based on duty cycle variation. The oscillation around the maximum power point (MPP) in steady-state can be better seen in Fig. 7 that shows the variation of *PPV* (*y* axis) with *IPV* (*x* axis) in that time interval.

One can see in Fig. 8 that the top waveform, the voltage in the intermediate DC bus presents a small second order ripple, typical of single-phase DC-AC converters, and that its average value is about 30 V. The waveforms in the bottom of Fig. 8 are the voltage and current in the AC side. It is shown that they are in-phase as expected for the desired unity (displacement) power factor operation.Fig.

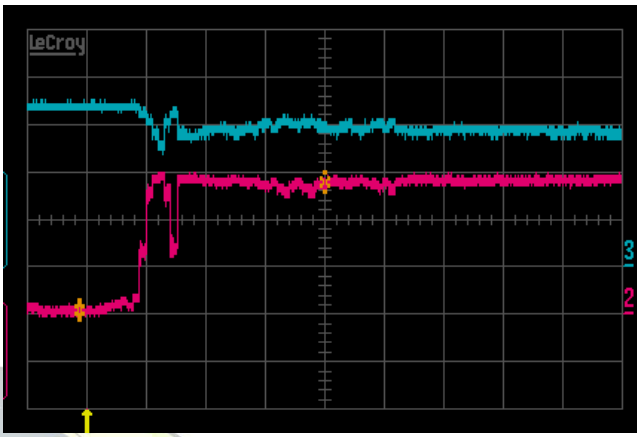

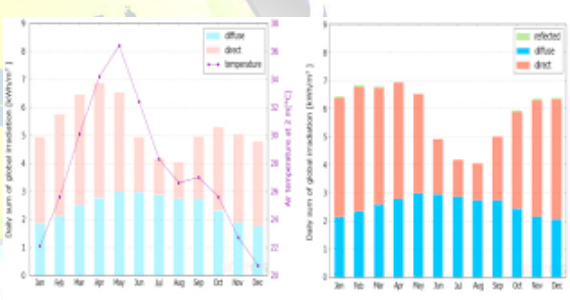

PPV-MP 23.4 W

Operation in the Grid-Connected Mode

The harmonic spectrum of the injected current is shown in Fig. 9. The FFT was calculated after getting all the data points experimentaly. The total harmonic distortion (THD) of the injected current was computed as 14.77% using numerical calculation. This is mostly due to the relatively large magnitude of the 3rd harmonic, which is not a switching harmonic, and therefore it is not affected by the output filter of the DC-AC converter. This harmonic could be minimized by introducing a dead-time compensation scheme which should also reduced the distortion seen at the positive zero crossing

Operation in the Stand-alone Mode

ISSN 2394-3777 (Print)
ISSN 2394-3785 (Online)
Available online at www.ijartet.com

International Journal of Advanced Research Trends in Engineering and Technology (IJARTET)
Vol. 5, Special Issue 12, April 2018

In the stand-alone mode, the DC-AC converter is controlled to regulate the voltage supplied to the load, leaving the intermediate DC bus voltage unregulated. In case the load power is larger than the PV power, the DC bus voltage will decrease, what should result in a reduction in the output voltage and eventual over-modulation by the closed loop control. A scheme to prevent overvoltage and damage to switches and DC capacitor when the power demanded by the load is lower than the power drawn from the PV panel is required. The conditions for this test are as follows: The PV panel operates with rated solar irradiance, *PPV-MP* ~ 23.4 W, and a resistive load of 13 Ω is placed at the output of the PV interface with a reference voltage of 15 Vrms. As the overvoltage is detected, the value of the duty cycle of the boost DC-DC converter is set to 0.35 and the MPPT routine resumes. In this case, as shown in Fig. 11, the voltage in the DC bus varies between a maximum value of 30 V, when the overvoltage protection is activated, and a minimum value of 28 V, with a certain period. These voltages are within the range required by the DC-AC converter to keep the voltage across the load regulated.

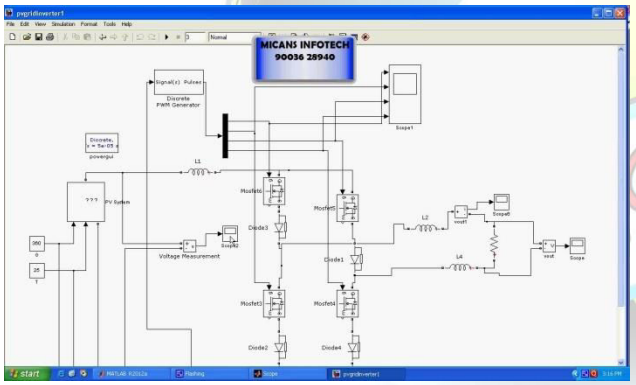

CONCLUSION

Modeling and stability analysis of a single-phase two-stage grid-connected photovoltaic system have been presented in this paper. (1) An integrated mathematical model including both DC-DC converter and DC-AC converter is developed to capture the dynamics of the system, also the nonlinear characteristic of the PV array is considered in the model; (2) An observer-pattern modeling method is applied to transform the system into time-invariant; (3) Critical controller parameters that influence the stability of the system are identified using eigenvalue sensitivity and eigenvalue loci plots. It is found that Ti1 is closely related to *l*3,4. The decrease in Ti1 makes *l*3,4 move to left in the s-plane and is disadvantageous to the stability of the system. The theoretical results have been validated by PSIM simulations.

This paper has discussed the implementation of a digital control system for a 2-stage PV inverter capable of operating in the grid-connected and in the stand-alone modes. The low power Texas Instruments Renewable Energy Developer's Kit (TI REK), which presents the required power converters, sensors and filters along with a F2808 C2000 control card has been selected. Some experimental results have demonstrated the effectiveness of the following techniques in steady-state and transient conditions: MPPT, protection against overvoltage in the intermediate DC bus, current injection in an AC grid with UPF.

REFERENCE

[1]Key World Energy Statistics, International energy Agency, 2012:[Online].
Available:
http://www.iea.org/publications/freepublications/publication/kwes.pdf

[2] J.M. Carrasco, L.G. Franquelo, J.T. Bialasiewicz, E. Galvan, R.C.P.Guisado, Ma.A.M. Prats, J.I. Leon and N. Moreno-Alfonso, "Powerelectronic systems for the grid integration of renewable energy sources: A survey," *IEEE Transactions on Industrial Electronics*, Vol. 53, No. 4, 2006, pp. 1002-1016.

[3] M. Calais, J. Myrzik, T. Spooner and V.G. Agelidis, "Inverters for single-phase grid connected photovoltaic systems – an overview," in 34th Annual IEEE Power Electronics Specialists Conference(PESC02), Vol. 4, pp. 1995-2000.

[4] M. Bhardwaj and S. Bharathi, "Implementing Photovoltaic Inverter System Using C2000 Microcontrollers on Solar Explorer Kit,". [Online].
Available:
ftp://ftp.ti.com/pub/dml/DMLrequest/Christy_FTP-10-3012/controlSUITE/development_kits/SolarExplorer_v1.0/SolarExplorer_PVInverter_F2803x/~Docs/PVInverter_F2803x.pdf

[5] F. Ishengoma, F. Schimpf and L. Norum L, "DSP-controlled Photovoltaic Inverter for Universal Application in

ISSN 2394-3777 (Print)
ISSN 2394-3785 (Online)
Available online at www.ijartet.com

International Journal of Advanced Research Trends in Engineering and Technology (IJARTET)
Vol. 5, Special Issue 12, April 2018

Research and
Education" in IEEE PowerTech, Trondheim, 2011, pp. 1-6

[6] M.A.G. de Brito, L. Galotto, L.P. Sampaio, G. de Azevedo e Melo and C.A. Cansein, "Evaluation of the main MPPT techniques for photovoltaic applications," *IEEE Transactions on Industrial Electronics.*, Vol. 60, No. 3, 2013, pp. 1156-1167y System with C2000 Micro-Controllers, 2009. [Online].
Available:
http://www.element14.com/community/docs/DOC-28359/l/alternative-energy-design-resources

[7] M. Calavia, J.M. Perié, J.F. Sanz and J. Sallán, "Comparison of MPPT strategies for solar modules," in International Conference on
Renewable Energies and Power Quality (ICREPQ'10), pp. 1-6.

[8] G.F. Franklin, J.D. Powell and M. Workman, Digital Control of Dynamic Systems, Ellis-Kagle Press, 3rd edition, 2006.
Cucchiella, F.; D'Adamo, I.; Gastaldi, M. Economic analysis of a photovoltaic system: A resource for residential households. Energies **2017**, 10, 814. [CrossRef]

[9]Kouro, S.; Leon, J.I.; Vinnikov, D.; Franquelo, L.G. Grid-Connected Photovoltaic Systems: An Overview of
Recent Research and Emerging PV Converter Technology. IEEE Ind. Electron. Mag. **2015**, 9, 47–61. [CrossRef]

[10]. Schimpf, F.; Norum, L. Effective use of film capacitors in single-phase PV-inverters by active power
decoupling. In Proceedings of the 36th Annual Conference on IEEE Industrial Electronics Society,
Glendale, AZ, USA, 7–10 November 2010; pp. 2784–2789.

[11]. Nižeti´c, S.; Papadopoulos, A.M.; Tina, G.M.; Rosa-Clot, M. Hybrid energy scenarios for residential
applications based on the heat pump split air-conditioning units for operation in the Mediterranean climate
conditions. Energy Build. **2017**, 140, 110–120. [CrossRef]

[12]. Xiong, X.; Chi, K.T.; Ruan, X. Bifurcation Analysis of Standalone Photovoltaic-Battery Hybrid Power System.
IEEE Trans. Circuits Syst. I Regul. Pap. **2013**, 60, 1354–1365.

[13].Deivasundari,
P.; Uma, G.; Poovizhi, R. Analysis and experimental verification of Hopf bifurcation in a solar
photovoltaic powered hysteresis current-controlled cascaded-boost converter. IET Power Electron. **2013**, 6, 763–773. [CrossRef]

[14]. Zhioua, M.; Aroudi, A.E.; Belghith, S.; Bosquemoncusí, J.M.; Giral, R.; Hosani, K.A.; Alnumay, M. Modeling,
Dynamics, Bifurcation Behavior and Stability Analysis of a DC–DC Boost Converter in Photovoltaic Systems.
Int. J. Bifurc. Chaos **2016**, 26, 1650166. [CrossRef]

[15]. Al-Hindawi, M.M.; Abusorrah, A.; Al-Turki, Y.; Giaouris, D.; Mandal, K.; Banerjee, S. Nonlinear
Dynamics and Bifurcation Analysis of a Boost Converter for Battery Charging in Photovoltaic Applications.
Int. J. Bifurc. Chaos **2014**, 24, 373–491. [CrossRef]

[16]. Abusorrah, A.; Al-Hindawi, M.M.; Al-Turki, Y.Mandal, K.; Giaouris, D.; Banerjee, S.; Voutetakis, S.; Papadopoulou, S. Stability of a boost converter fed from photovoltaic source. Sol. Energy **2013**, 98, 458–471. [CrossRef]

[17]. Li, X.; Tang, C.; Dai, X.; Hu, A.; Nguang,
S. Bifurcation Phenomena Studies of a Voltage Controlled Buck-Inverter Cascade System. Energies **2017**, 10, 708.

BIOGRAPHY

C.Selsiya P.G Scholar (M.E., P.E.D)
P. A.College of Engineering and Technology, Pollachi.
IEEE-Member